OPTIMAL POWER CONTROLLER BASED VOLTAGE AND FREQUENCY CONTROL OF DG UNIT IN AN ISLAND MODE MICROGRD USING HYBRID DIFFERENTIAL EVOLUTION.

1.Mothi Ram.B
S.R.K.R.Engineering College, Bhimavaram,India.
09849728366,mothiramsrkreee@gmail.com

2. Dr.Ravi Srinivas.L, Professor &Head,
Gudlavalleru Engineering College,Gudlavalleru.India.
09490629536, lravisrinivas@gmail.com

Abstract:
The article focuses on placing the typical Power-Electronics-Interfaced Distributed Generation (DG) systems on optimal power control mode in island mode microgrid operation which is supplemented by a new online intelligent technique. It also entails enhanced power quality that the DG system supplies which is cut off from the conventional grid. At a time when load shift occurs in the microgrid, the estimation of primary execution parameters viz., controlling voltage and frequency of DG units; steady-state as well as dynamic response; and total harmonic distortion (THD) and power quality of the microgrid is done under island mode as well as the load changing state. In contrast to the composition of a synchronous reference frame (SRF) and regular PI controllers, DG system controller consists of an internal current control loop, besides an external power control loop. In the current paper, the DG system voltage and frequency are controlled by implementing Vf' control mode by the power controller in the DG system. The optimal tuning of the most traditional proportional-integral (PI) controller of the power controller is done by applying a smart technique i.e. Hybrid Differential Evolution (HDE). The system model and simulation outputs developed by applying MATLAB/Simulink software platform indicate a better performance for the new power controller in resolving power quality issues. Better results are obtaining with HDE method when compared with Differential Evolution (DE).

Keywords: *Microgrid, Distributed Generation (DG),Island mode, Load changing mode, Power controller, Current controller, Hybrid Differential Evolution (HDE).*

I. Introduction.

A microgrid comprises a set of DG systems and loads, which is linked to an electrical distribution system through Voltage Source Inverter (VSI). In view of a sudden change in load demand, the microgrid acts like a complementary infrastructure to the conventional grid. A microgrid functions in utility grid-connected mode as well as in island mode. On top of that, renewable energy sources emerge as alternatives that offer power and flexible extension to the maingrid [1]. However, the renewable energy sources have close proximity with Pulse-Width-Modulation(PWM) that is based on VSI system having nonlinear voltage-current features. Such electronic devices generate switching frequency at a higher rate. In fact, the power quality issues from the consumer's perspective are influenced by the above factors **[**2].

Fig.1 exhibits a microgrid. The power quality issues can only be effectively tackled by applying a robust control mechanism to allow the DG systems to attain functional connection with the utility grid. In essence, the PWM-VSI system based current control mechanism is of critical importance in the realm of power converters. Basically, current regulators comprise of the feedback current type PWM nonlinear mechanism and the nonclosed loop voltage type PWM linear mechanism having connection with internal current closed loop [3].

In a VSI-based nonlinear system with three-phase grid connection, Hysteresis Current Control (HCC) is widely employed that usually generates PWM signals. The generated PWM signals create more ripples in current i.e high total harmonic distortion (THD) because of its control delay and failure to produce zero voltage [4]. Due to its ability to offset the current error by the PI-controller, SVPWM based controller is a satisfactory controller for linear current control. The SVPWM based controller compensates and produces PWM signals independently which results in minimum current ripple, outstanding steady-state response, and a non-disturbed sinusoidal waveform [5].

In the current scenario, most of the researchers tend to examine voltage and frequency controls from the prism of internal current control loop in a microgrid to regulate the set parameters**.** Typically, a DG unit must be designed to deliver maximum power with equally high stability levels [6]. The power controller

approach applied in the Microgrid system can generate dynamic performance, in general and high performance in load sharing distribution system, in particular [7]. But the above process needs self-moving control parameter tuning to optimize the operation during sudden changes.

In fact, there are a host of techniques that handle optimization and nonlinear challenges, which are categorized based on the nature of search space or objective function. In *Linear Programming* (LP), just the linear objective function is used, in addition to achieve linear parity and reduce inequality constraints. In *Nonlinear Programming* (NLP), nonlinearity objective function and constraints are used, which is however inferior to the results obtained when all limitations remain linear. This condition is known as Linearly Constrained Optimization. The difficulties arising out of ambiguity can be resolved by application of probability functions of variables through *Stochastic Programming, otherwise known as Dynamic Programming* (DP) [8]. It has widespread usage in tackling optimization issues, wherein the numerical results obtained through computation enhance the parameters optimized through autonomy. In [9-10], in PSO, velocity updating can be of minuscule value. But, with minute cognitive and social components, it fails to recover to high value, besides failing to recover the lost search capabilities in a few generations. If majority of particles face constriction by local minima, then, the evolution process results in stagnation in due course of time. To obviate the trend, the mutation operator is applied to Differential Evolution (DE) for preventing stagnation and avoids early abortion [11-13]. But DE offers a quick convergence speed in the one-to-one competition. But, this quick convergence produces a premature convergence. This snag can be conquered by utilizing a large size population. But, it requires more execution time. Hence it is sought to counter such problems by developing the algorithm Hybrid Differential Evolution (HDE) [14-16].

The residual section of this article is categorized into five sections. A demonstration of a VSI-led three-phase grid-connected mathematical modeling is done in section II. Section III explains the role of 'Vf' control approach in tackling power quality issues in a microgrid, while a detailed description of the suggested control approach is given in section IV. Section V examines the MATLAB simulation outputs. Section VI contains the conclusion.

Fig.2 represents the grid-connected 3-phase VSI alongside an LC filter, wherein 'Ls, Rs, C' represent the proportionately combined dosage of inductance, resistance and capacitance in the filter.

II. Mathematical Modeling of Three-Phase on grid Mode -VSI systems.

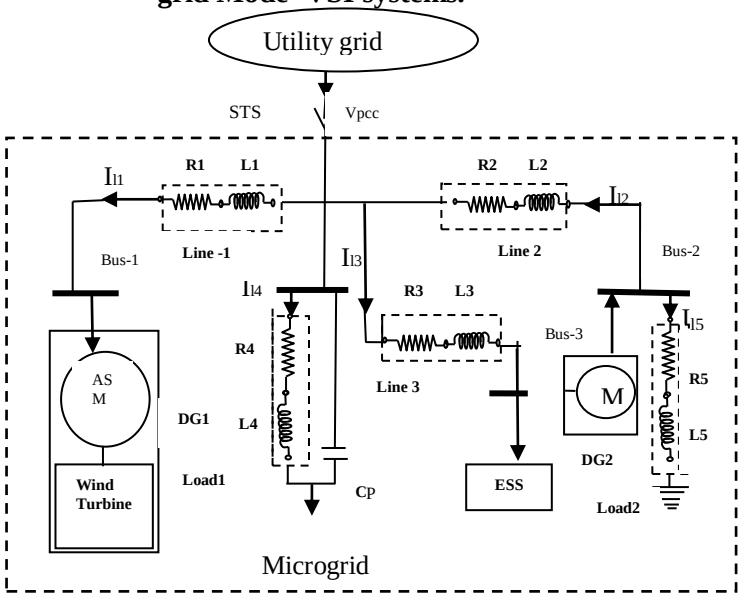

Fig.1 Example of Microgrid system.

The voltage of the utility grid is represented by 'Vs'. The Insulated Gate Bipolar Transistor (IGBT) type switching device is used in a DC-AC converter. The "abc" reference frame represents the state-space representation approach as given below (1):

$$\frac{d}{dt}\begin{bmatrix} i_a \\ i_b \\ i_c \end{bmatrix} = \frac{R_s}{L_s}\begin{bmatrix} i_a \\ i_b \\ i_c \end{bmatrix} + \frac{1}{L_s}\left(\begin{bmatrix} V_{sa} \\ V_{sb} \\ V_{sc} \end{bmatrix} - \begin{bmatrix} V_a \\ V_b \\ V_c \end{bmatrix}\right) \quad \text{..... (1)}$$

Above equation can be transformed into '*dq'* frame by Using Park's transformation, it is expressed as $i_{dq0} = T i_{abc}$ and given by (2)

$$\frac{d}{dt}\begin{bmatrix} i_d \\ i_q \end{bmatrix} = \begin{bmatrix} -\frac{R_s}{L_s} & \omega \\ -\omega & -\frac{R_s}{L_s} \end{bmatrix}\begin{bmatrix} i_d \\ i_q \end{bmatrix} + \frac{1}{L_s}\left(\begin{bmatrix} V_{sd} \\ V_{sq} \end{bmatrix} - \begin{bmatrix} V_d \\ V_q \end{bmatrix}\right) \quad \text{..... (2)}$$

Where, 'T' and'ω' represent the transformation matrix and angular frequency, respectively.

III. 'Vf' Control Technique:

As opposed to big-sized generators, DG units require energy sources such as high-speed source like micro-turbine generator, variable speed source like Wind energy and direct power transformation source like photovoltaic and fuel cells. Hence, it is important that a typical DG unit interface using VSI is connected to main grid for providing smoother action. Fig.2 shows

the DG unit based on "Vf" controller of the Power-Electronics-Interfaced VSI which is linked to the control structure, thereby signifying the dependence of controlled action of the DG unit upon the control mode of the Electronics-Interfaced inverter.

In microgrid action, it is important to make sure the smooth transformation among the microgrid action modes, also hold stability, controlling the voltage as well as frequency in relation to the load demand in autonomous operation mode. The 'Vf' control mode is accepted by more than one DG units when the DG unit maintains voltage and frequency within limits in respect to the load requirement under this mode. The computation of microgrid frequency is done while using Phase-Locked-Loop (PLL) and voltage Vrms in [6].

$$V_{rms}=\sqrt{V_d^2+V_q^2} \quad \text{---------- (3)}$$

IV. Proposed Power Control Technique:

This controller aims at improving the non-distributed supply waveform while operated in control objective mode. The 'Vf' designed controller based on twin PI controllers is illustrated in Fig.3, thereby signifying the utility of an external power controller for producing current vectors i_d^* and iq^* in that order. As a result, a moderately slow modification of the reference current trajectory is expected to create higher quality inverter output power, thus attaining the set control levels. In DG unit based SVPWM-VSI, the 'Vf' controller is modeled on HDE, DE and PSO algorithms for optimizing the PI controller that identify the primary control parameters like system voltage and frequency in both autonomous and load changing states**.** Here, system voltage is controlled by the power controller, besides the frequency based in the reference values (V_{ref} as well as f_{ref}). Further, it applies all optimization techniques to provide optimum control values for generating the reference current vectors. So, two PI controllers in a'dq' frame are represented by reference current vectors as:

$$i_d^*=(V_{ref}-V)(K_{pv}+K_{iv}/s) \quad \text{---------- (4)}$$

$$i_q^*=(f_{ref}-f)(K_{pf}+K_{if}/s) \quad \text{---------- (5)}$$

(i).Current control technique:

The projected controller is designed to ensure near-perfect measurement of output current of the inverter in the form of short transient. The implementation of the current control loop in the internal current controller on the sub-stratum of a 'αβ'-stationary frame is illustrated in Fig.4. The phase angle of voltage is detected by PLL block for securing 'dq' reference frame. In fact, two PI controllers are applied to reduce error in current, while the steady state and dynamic response is enhanced by application of dynamic inverter current loop and the forward path grid voltage. It results in the output values of this controller matching the voltage reference values in the park's transformation. Thereafter, converted into 'αβ'- stationary frame, the reference voltage values in $'Park's'$ transformation are created by controller, which is then combined with six pulses so that the SVPWM triggers the IGBT inverter. From Eq. (2), the voltage reference values are given in the synchronous reference frame:

$$\begin{bmatrix}V_d^*\\V_q^*\end{bmatrix}=\begin{bmatrix}-K_p & -\omega L_s\\ \omega L_s & -K_p\end{bmatrix}\begin{bmatrix}i_d\\i_q\end{bmatrix}+\begin{bmatrix}K_p & 0\\0 & K_p\end{bmatrix}\begin{bmatrix}i_d^*\\i_q^*\end{bmatrix}+$$

$$\begin{bmatrix}K_i & 0\\0 & K_i\end{bmatrix}\begin{bmatrix}X_d\\X_q\end{bmatrix}+\begin{bmatrix}V_{sd}\\V_{sq}\end{bmatrix} \text{------- (6)}$$

Where the character '*indicate reference values,

$$\frac{dX_d}{dt}=i_d^*-i_d \text{ as well as } \frac{dX_q}{dt}=i_q^*-i_q$$

Clarke's transformation is used to to convert Equation (6) into 'αβ'-stationary frame [9].Further, LPF can be used to obtain the inductor current. The following equation represents the first-order transfer function of LPF (7).

$$f_l=\frac{f}{1+sT_i} \text{-------- (7)}$$

Where $'f_l'$ is the filtered value; 'f' represents the input value of filter; and 'T_i is the time constant.

(ii). Standard Differential Evolution (DE) Algorithm:

Nonlinear and non-differentiable, non-discrete space function with real-value parameters is formulated by Storm and Price[12-13].This uses the variance of entity vector pairs randomly sampled to steer the mutation constant instead of utilizing functions other than EA's methodology for probability distribution.

The distribution of the dissimilarity between randomly measured entity variables is observed through the vector distribution of such entity vectors.

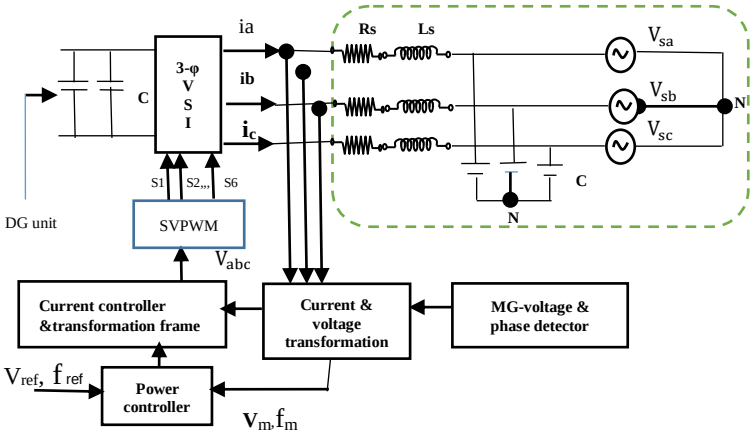

Fig.2 Three-Phase grid-connected VSI model.

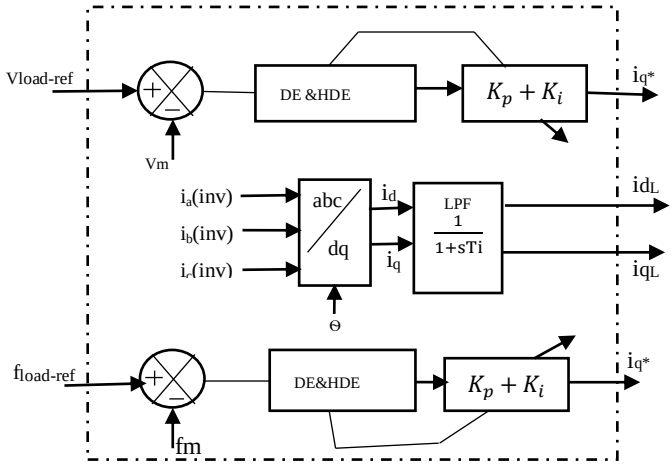

Fig.3 The Proposed Power Controller

.

The key benefits of DE detailed in [15]. An optimization process comprises of 'D' parameters that can be viewed by a D-dimensional matrix. In DE, at the begining a population of 'NP' solution vectors is created arbitrarily. This population is effectively improved across 'G' generations by utilizing crossover and selection, mutation operators to attain best available solution [14] .The DE algorithm's principal steps:

Phase1: Initialization: The randomly chosen value of the control variable population is created from its corresponding possible values.

$$X_{j,i}^{(0)} = X_j^{min} + \mu\left(X_j^{max} - X_j^{min}\right), i = 1, \ldots., NP, \quad J = 1, \ldots \ldots D \text{ ---------- (8)}$$

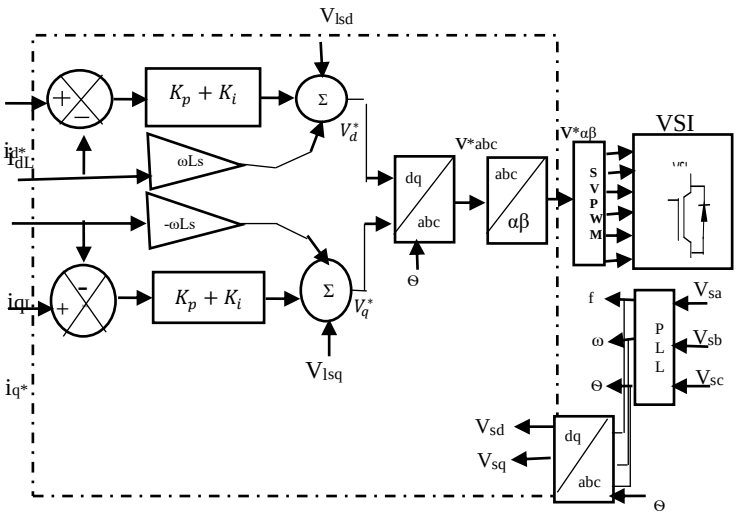

Fig.4 The Current Controller Scheme.

Where μ_j marks an integer number that is routinely spread within range [0 1].

Phase2: Mutation: The mutation constant (F) generates mutant variable X_i^l by spreading randomly selected variables X_a with the variance of two other arbitrarily preferred vectors X_b and X_c, as described in (9):

$$X_i^{l(G)} = X_a^{(G)} + F\left(X_b^{(G)} - X_c^{(G)}\right), i = 1, \ldots . NP \text{--- (9)}$$

Here X_a, X_b and X_c are arbitrarily chosen variables within the population of the 'NP', and a novel for every parent vector is chosen for a set of a≠ b ≠ c. The mutant factor inside the [0-1] scale, which determines the perturbation sum in the scaling process.

Phase3: Crossover (CR): In this step, in order to add more individuals, possibly in the next generation, a binomial distribution is applied to cull the perturbed individual of X_i^{11} and the current individual of $X_{j,i}^{1(G)}$ to complete the crossover operation and create scions.

$$X_{j,i}^{11(G)} = \begin{cases} X_{j,i}^{1(G)}, \text{if } r \le CR, i = 1 \ldots . NP, j = 1 \ldots \ldots . D. \\ X_{j,i}^{(G)}, \text{otherwise} \end{cases} \text{--- (10)}$$

Here i=1…….NP, g=1…..n; and the CR ϵ [0-1] .

Here"r" signifies a random number that is distributed evenly in range [0-1], build a new value for each of j.'q' is an arbitrarily selected index $\epsilon\{1\ldots$ NP$\}$ which guarantees that the test variable contains no less than one parameter of the mutant constant (F). The convergence element is in the [0-1] scale,which controls population diversity.

Phase4: S*election*

The selection method produces the population by preserving the appropriate combination of present and post vectors according to equation (11).

$$X_i^{(G+1)} = \begin{cases} X_i^{u(G)}, & \text{if } f\left(X_i^{u(G)}\right) \le f\left(X_i^{(G)}\right) \\ X_i^{(G)}, & \text{otherwise} \end{cases},$$

$i = 1, \ldots, NP.$ ---------- (11)

For a specified number of iterations, the above measures are replicated to maximize their health as they look for the answer space to discover the right values.

(iii).Proposed Standard Hybrid Differential Evolution (HDE) Method:

The DE is outstanding among the most unrivaled calculations for development. In view of a stochastic operation, this is an uncomplicated technique in which feature parameters are defined as floating-point variables.DE's computational algorithm is easy to grasp and implement. Users are expected to set only a few parameters in this algorithm. The fitness of descendants is one-to-one comparison to that of the parent in DE. Chiou and Wang [16–19] had built up an HDE to solve these difficulties by adding exodus process to the special version of DE to avoid using vast popualace.

Phase5: Function proposed for migration:

A migration feature is common to recreate a novel va ried community of individuals in order to efficiently bring better research to the quest spaces and the the s election burden to a minimal point. The novel populations are capitulated based on the best individual X_b^{G+1} . The h^{th} gene of the i^{th} individual is as per follows (12).

$$X_{hi}^{G+1} = \begin{cases} \text{round}\left(X_{hb}^{G+1} + \rho 1\left(X_{h\,min} - X_{hb}^{G+1}\right)\right), & \text{if } \rho 2 < \frac{X_{hi}^{G+1} - X_{h\,min}}{X_{h\,max} - X_{h\,min}} \\ \text{round}\left(X_{hb}^{G+1} + \rho 1\left(X_{h\,min} - X_{hb}^{G+1}\right)\right), & \text{otherwise} \end{cases}$$

---------- (12)

Here $\rho 1$, $\rho 2$ are numbers generated randomly are distributed uniformly within the framework of [0, 1]; $i = 1. \ldots\ldots NP$; $h = 1\ldots\ldots nc$.

Phase 6) Steps 2–5 are repeated until the maximum number of iterations or the desired fitness is reached.

(iv).Fitness Function (FF).

In the present paper, based on ITAE, Simpson's 1/3 rule is applied to complete evaluation of the controller's objective function. For instance, the ISE as well as ITSE are more aggressive since the error will be square which results in the consideration of the negative errors. The IAE is also insufficient than ITAE, which gives a practical error high, since this error is a product with the time. The ITAE method with example can be found in [21-22].

The ITAE index is determined by the mathematical formula is given as (13).

$$\text{ITAE} = \int_0^\infty t|e(t)|dt \quad \ldots\ldots\ldots\ldots (13)$$

In such a scenario, 't' represents time, while e (t) represents the error between the reference value and the controlled value.

(v).Criteria for Stopping.

Typically, an optimal searching algorithm is stopped at the completion of all iterations or at the attainment of best fitness value. In this study, we have taken the total number of iterations for minimizing the objective function so that best power control parameters are obtained. Table 1, 2 that illustrates the DE, HDE searching algorithm parameters are used under island as well as load changing state, in both states the number of populations as well as iterations are set to 30 and 50, and minimum and maximum of the power control parameters Kpv, Kiv and Kpf, Kif searching spaces are set to [-20 0], [0 5e-3],and [0 30],[0 5e-3], respectively [9]. In the present paper, a single DG unit microgrid model is simulated, besides independently creating each searching algorithm and its objective function in relation to each control objective. The execution parameters of the applied DE, HDE are presented in a detailed manner.

Table 1: The applied DE Parameters under Island mode.

DE parameter description	Kpf	Kif	Kpv	Kiv
Acceptable tolerance (P.U)	±0.01	±0.01	±0.1	±0.1
Crossover factor(CR)	0.8	0.8	0.8	0.8
Mutation Constant(F)	0.3	0.3	0.3	0.3
Under load changing mode				
Mutation Constant(F)	0.2	0.2	0.2	0.2

Table 2: The applied HDE Parameters under Island mode.

HDE parameter description	Kpf	Kif	Kpv	Kiv
Acceptable tolerance (p.u.)	±0.01	±0.01	±0.1	±0.1
Crossover factor(CR)	0.9	0.9	0.9	0.9
Mutation constant(F)	0.6	0.6	0.6	0.6
Under load changing mode				
Mutation constant(F)	0.9	0.9	0.9	0.9

In above-searching algorithms, the ITAE function is executed individually on voltage and frequency control objectives ('Vf'). Figures.5, 6, 7, and 8 show frequency and voltage control objectives under island and load changing modes, while the results represent the variations between reference value and the measured value of objective functions spread across a specific time period with the computation done by applying Simpson 1/3 rule. From the above results it is observed that the error reduces rapidly with a total number of iterations, and the result is constant towards the end.

In the present paper, for both island and load changing modes, the power control parameters for DE, HDE reside at the optimum values listed in Table 3, 4.

Table3:DE 'Vf' Controller Parameters.

Control parameters	Autonomous mode	Load changing state
Kpv	-2.036244751266294	-1.623631315683298
Kiv	5.000000000000000e-004	1.595014561243700e-04
Kpf	22.018723770417150	27.877908695616831
Kif	2.666064278086038e-005	1.749918829924044e-04

Table 4:HDE 'Vf' Controller Parameters.

Control parameters	Autonomous mode	Load changing state
Kpv	-2.043191720212568	-1.758762896305792
Kiv	1.079730358761263e-004	5.000000000000000e-004
Kpf	23.604902624982547	30
Kif	1.157893151233367e-004	4.999999999934847e-004

V. Simulation Results

The grid-connected three-phase VSI system is modeled by applying MATLAB/Simulink, besides new controller as exhibited by Fig.2. The execution of DE, HDE algorithms are done in MATLAB in the form of an M-file with the following specifications : Rs=1.4Ω, Ls=5mH, frequency (f) =50Hz, filter capacitance 'C'=1500μF; the DG Unit side input capacitor = 5000μF. Beisdes, it uses a single DG Unit of 50kW capacity. Typical internal current controller parameters are represented as K_P=12.656 and Ki=0.00215 [9]. The switching frequency and sampling frequency of SVPWM based current control is 10 kHz and 500 kHz. Exhibition of searching algorithm outputs is represented in per-unit (p.u) system that validates the following objects:

(i). Voltage as well as the Frequency Control:

In Fig.2, microgrid model is established through MATLAB/Simulink for making assessment of the proposed power (Vf) controller in the discussed online tuning algorithms. Operated in ON-grid mode, the voltage as well as frequency of the microgrid is developed by the main grid, which is responsible to keep within their tolerance. The microgrid transforms to the autonomous mode at 0.6s. The single DG unit consists of the power ('Vf') controller developed on the basis of DE, HDE stochastic based online tuning algorithms to alleviate the voltage reduction and eliminate a large frequency variation due to sudden transfer to autonomous modes or load changing mode. In both modes of operation, as given in (4), (5), the 'V'_{ref}, and 'f'_{ref} of the designed controller are fixed to 1 p.u. Fig.11 and Fig.12 represent the controlled voltage as well as the frequency of the proposed controller applied on above said stochastic optimization searching algorithms in autonomy mode at 0.6s. This mode fixes the load real power (P)-reactive power (Q) at 4.66 p.u and 1.45p.u as shown in Fig.9 and Fig.10. In Fig.11 the voltage is reduced peak value 0.934 p.u at 0.633 s and stable at 1.01p.u at 0.7 sec in DE, and 0.9345 p.u at 0.633 s and stable at 1.009 at 0.7sec in HDE. In same mode, in Fig.12 the frequency reach peak value 1.0095 p.u at 0.658s and stable at 1.0001 p.u at 0.74 sec in DE, and 1.0085 p.u at 0.656s and stable at 1.0001 p.u at 0.74 sec in HDE. In Fig.13.active power reduced peak value 4.4174 p.u at 0.636s in DE, 4.432 p.u at 0.636s in HDE but settled at 4.66 p.u at 0.715s in DE, at 0.71s in HDE. In Fig.14 the reactive power decreased peak value 1.3735p.u at 0.636 s in DE, and 1.378 p.u at 0.636s in HDE, but settled to 1.45 p.u at 0.71s in DE and HDE. At this point of time, as the above two stochastic searching algorithms begin searching to find new optimal power control parameters, the designed power controller resultantly transform into autonomy mode, thereby generating voltage and frequency to the tune of 1.004p.u at 0.68s and 1.0001 p.u at 0.72s, and real and reactive power to the tune of set value at 0.69s and 0.7s, respectively.

In load changing state, the real power as well as reactive power is decreased to 4.5 p.u and 1.4 p.u at 1.8s shown in Fig 9 and Fig.10. In this mode, as shown in Fig.11 the voltage rises to peak value to 1.05 p.u at 1.8s but settle at 1.026 p.u at 1.85 in DE, and 1.045p.u at 1.8s and settle at 1.025p.u at 1.85s in HDE. In Fig 12, the frequency reduced to 0.9945 p.u at 1.848s and reaches 1.0p.u at 1.89s in DE, and reduced to 0.9965 p.u at 1.846 and reached to reference value at 1.88s in HDE. In Fig 13. the active

power reduced peak value 4.473p.u at 1.853s in DE,4.475p.u at 1.852s in HDE, but reach set value at 1.865s in DE,1.86s in HDE.In Fig.14 the reactive power decreased peak value 1.391p.u at 1.852s in DE and1.392p.u at 1.852s in HDE, but reach set value at 1.88s in DE and 1.87s in HDE.

Hence, above two stochastic searching algorithms once again commence their search operations so that the designed power (Vf) controller generates optimal parameters in a bid to minimize errors in fitness functions.

Fig.11 and Fig.12 shows the designed power controller still provides outstanding response and remains the system voltage and the frequency of the DG unit equal to 1.004p.u as well as 1.0001 p.u, respectively.

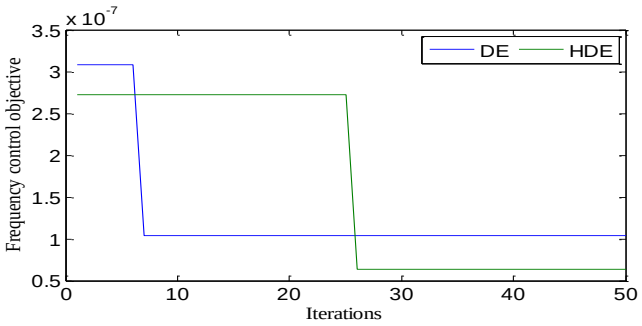

Fig.5. Fitness values of the Frequency control objective in Island mode .

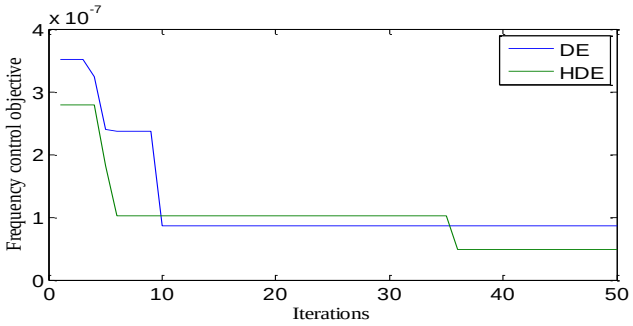

Fig.6.Fitness value of the Frequency control objective under load changing state.

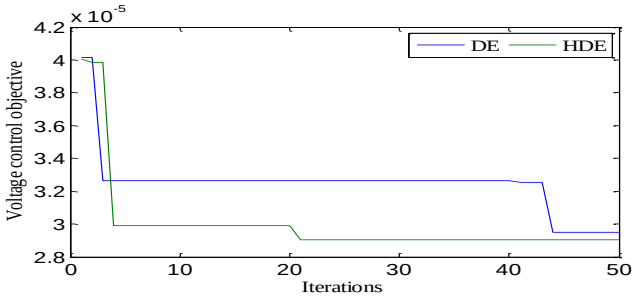

Fig. 7 Fitness values of the Voltage control objective in Island mode.

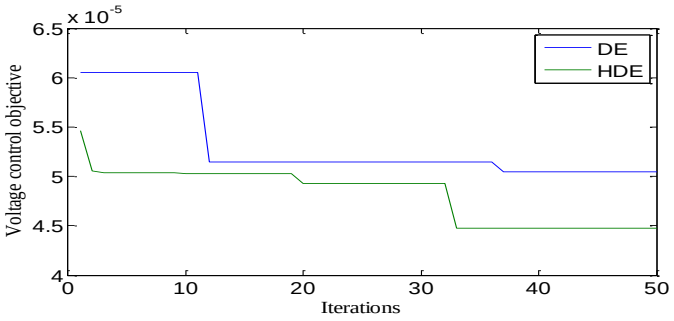

Fig. 8 Fitness values of the Voltage control objective in load changing state.

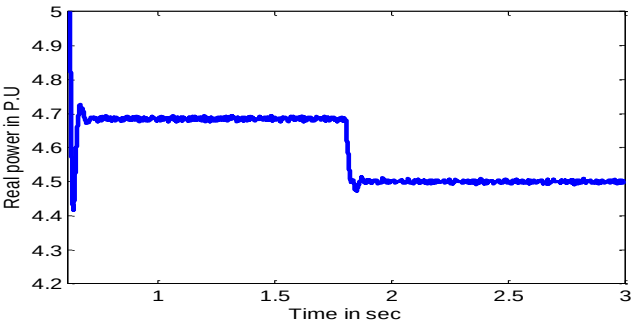

Fig.9 The Active load

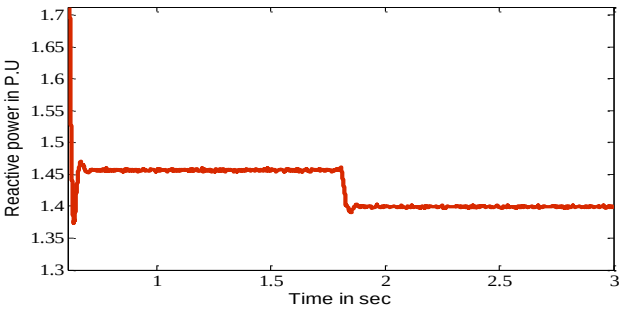

Fig.10. The Load Reactive power

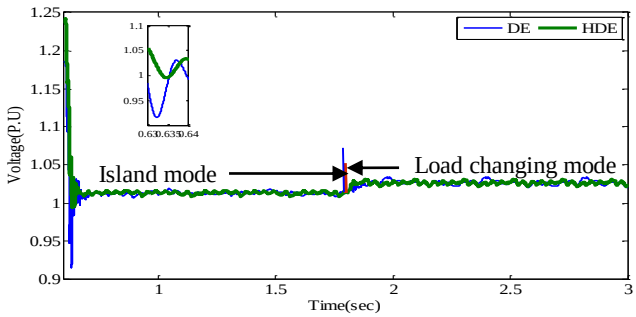

Fig. 11. The microgrid Voltage Regulated by Vf Controller

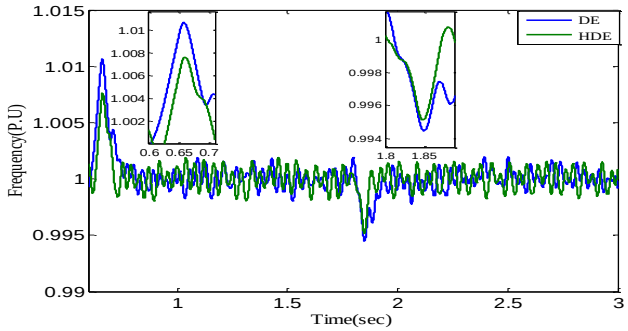

Fig. 12 The microgrid Frequency Regulated by Vf Controller

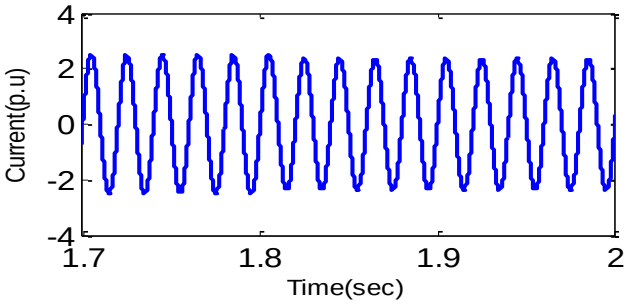

Fig.16 The dynamic response when the load changing state at 1.8sec

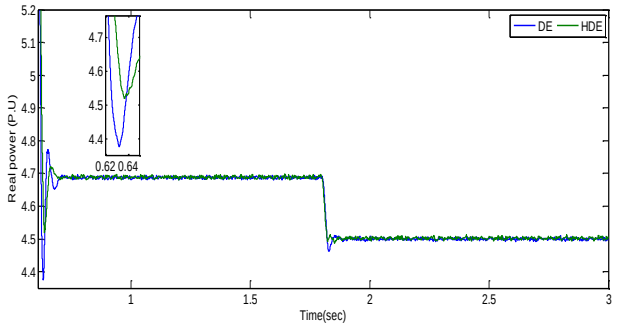

Fig. 13 The Real power supplied by DG by Vf Controller

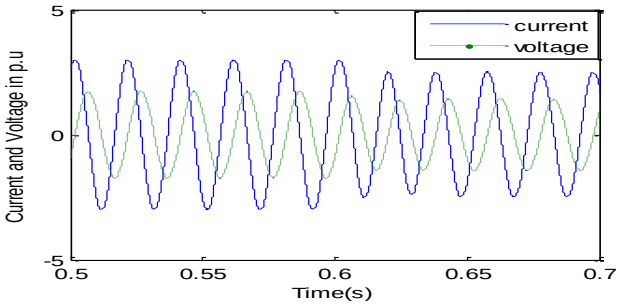

Fig.17 Transient and Steady-state response in island mode

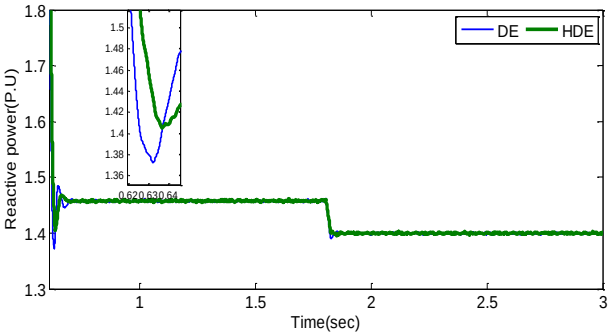

Fig. 14 The Reactive power supplied by DG by Vf Controller

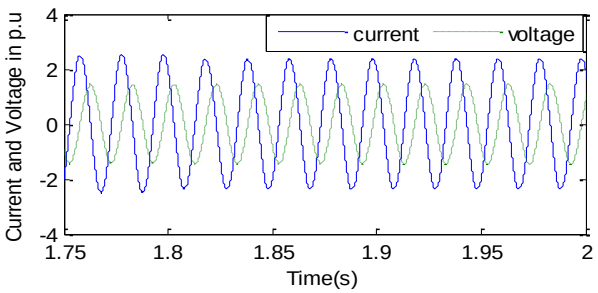

Fig.18. Transient and Steady-state response during load changing state.

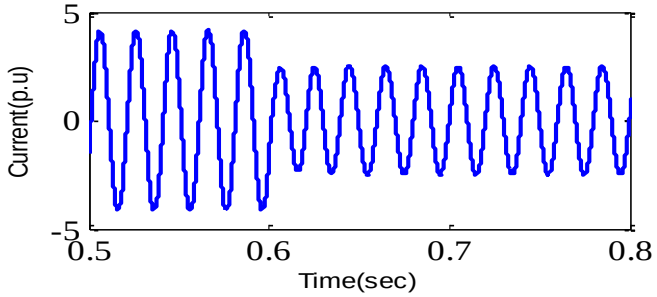

Fig.15 The dynamic response when the microgrid is island at 0.6s.

outstanding response and remains the system voltage as well as frequency of the DG unit equal to 1.024p.u.as well as 1.00015p.u,from Table 2,it is observed that the power ('Vf') controller is proposed technique regain the DG unit voltage as well as frequency match to their reference ranges surrounded by ±0.1(Volts) and ±0.01(0.5 Hz).

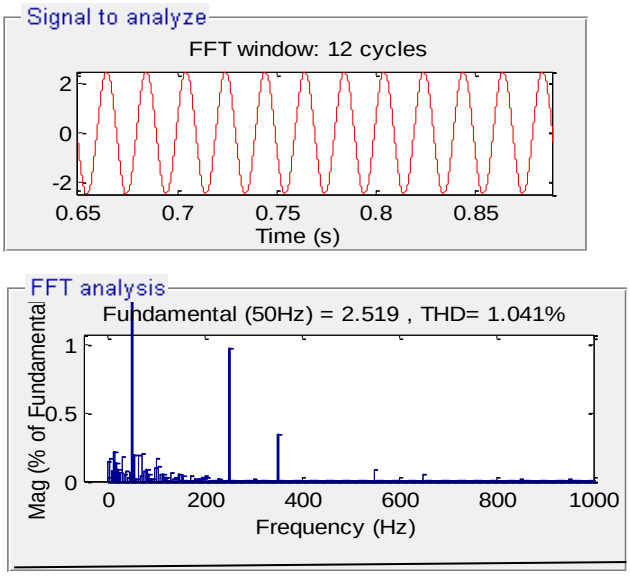

Fig.19 Spectrum of the VSI load current of the island mode.

Table.5: Comparison of THD's

Algorithm	THD (%)	
	Island	Load Changing State
PSO[9]	1.79	1.04
DE	1.05	1.03
HDE	1.041	1.024

(ii).Steady-State and Dynamic Behavior:

Testing of the output current of the DG unit is done in two modes while validating changing behavior of the designed power controller. First, the microgrid starts in autonomy mode at 0.6s, while movement towards load changing state starts at 1.8s. The simulation output line current of the inverter is exhibited in fig.15 and fig 16. The transient time in both modes is very short as well as line current reaches a constant value below two cycles.

In figures 17 & 18, the microgrid phase voltage behavior in transient and steady-state is exhibited in the presence of the line current of the inverter in autonomy mode as well as load changing state. In this article, an output of the filter is used to reduce switching harmonics by applying a low pass filter with low cut-off frequency so that fading is utilized for the harmonic content of the'dq'current vectors, thereby ensuring that the outputs waveforms remain non-distributed sinusoids having unity power factor.

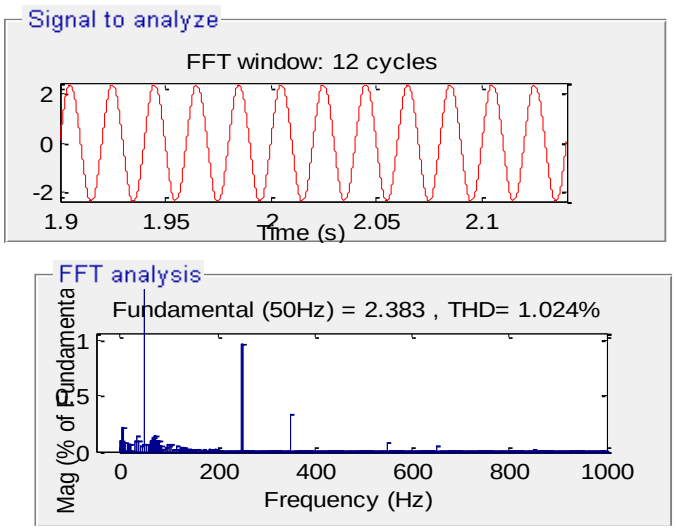

Fig.20 Spectrum of the VSI load current during the load

Figures.19, 20 illustrates the spectrum of the line current under autonomous mode as well as load changing state. The THD (%) values for various optimization searching algorithms are given in Table 5.which are less than 5% THD acceptable in IEEE Standard 1547-2003[23].

VI. Conclusion.

In essence, the present work has effectively proposed a novel 'Hybrid Differential Evolution (HDE)' optimization method. In fact, an internal current control is encased in a novel power control mode, while the demonstration for the external power control in the designed systems is done through computer simulation by using MATLAB/Simulink software. The control of the microgrid voltage and frequency is done in autonomous mode and state of load changing by executing an optimal online tuning strategy through stochastic online searching algorithms, which are executed and incorporated into the power (Vf) controller. In this work, power quality of the MG and dynamic, steady state, and the harmonic current of the inverter is explored using the projected controller. Above two online tuning searching algorithm results, HDE searching algorithm output gives better performance when compared with DE optimization techniques. The simulation output showed that the designed controller offers a proficient behavior for controlling the micro-grid voltage, besides ensuring the desired frequency as well as attaining shorter duration transient time having an tolerable THD level. The proposed

controller can be utilized in one or more DG systems in a microgrid that has the potential to reduce power-sharing problems by halve.

References

[1]. Lasseter RH. "*Microgrids*" Power engineering society winter meeting", vol.1. IEEE; 2002. p. 305–8.

[2] .Strzelecki R, Benysek G. "*Power electronics in smart electrical energy networks*". London: Springer, Verlag; 2008.

[3]. Qingrong Z, Liuchen C. "*Study of advanced current control strategies for three-phase grid-connected PWM inverters for distributed generation*". In: Proceedings of 2005 IEEE Conference on Control Applications, CCA 2005;2005. p. 1311–16.

[4]. Bong-Hwan K, Byung-Duk M, Jang-Hyoun Y." *An improved space-vector-based hysteresis current controller*". IEEE Trans Ind Electron 1998;45(5).

[5]. Kazmierkowski MP, Malesani L. "*Current control techniques for three-phase voltage-source PWM converters*": a survey. IEEE Trans Ind Electron 1998;45(5):691–703.

[6]. Wei D, Xisheng T, Zhiping Q. "*Research on dynamic stability of hybrid wind/PV system based on micro-grid*",In: International Conference on Electrical Machines and Systems, ICEMS 2008; 2008. p. 2627–32.

[7]. Wang Y, Lu Z, Yong M. "*Analysis and comparison on the control strategies of multiple voltage source converters in autonomous microgrid"*. In: 10th IET International Conference on Developments in Power System Protection (DPSP 2010). Managing the Change. p. 1–5.

[8].Nocedal J, Wright S. "*Numerical optimization*". Springer Verlag; 1999.

[9].Waleed Al-Saedi, Stefan W. Lachowicz, Daryoush Habibi, Octavian Bass." "*Voltage and frequency regulation based DG unit in an autonomous microgrid operation using Particle Swarm Optimization*" Intr Electrical Power and Energy Systems 742–751, 2013.

[10].M. A. Hassan and M. A. Abido, *Member, IEEE*, "*Optimal Design of Microgrids in Autonomous and Grid-Connected Modes Using Particle Swarm Optimization*", IEEE Transactions on power electronics, vol. 26, no. 3, march 2011.

[[11].R. Storn and K. Price, "*Minimizing the real functions of the ICEC '96 contest by differential evolution*,"IEEE Conference on Evolutionary Computation, Nagoya, pp.842-844, 1996.

[12]. Sk. Minhazul Islam, Swagatam Das, Saurav Ghosh, Subhrajit Roy, and Ponnuthurai Nagaratnam Suganthan, "*An Adaptive Differential Evolution Algorithm With Novel Mutation and Crossover Strategies for Global Numerical Optimization*" IEEE transactions on systems, man, and cybernetics—part b: Cybernetics, vol. 42, no. 2, April 2012.

[13].Dr.L.Ravi srinivas,B.Mothiram" *Voltage and Frequency Control of Distribution Generation Unit in an Island Mode Microgrid Using Differential Evolution*"IEEE conference on Second International Conference on Intelligent Computing and Control Systems (ICICCS) 2018. Conference Location: Madurai, India, Date of Conference: 14-15 June 2018,Date Added to IEEE *Xplore*: 11 March,2019.

[14]. Ching-Tzong Su, Chung-Fu Chang & Chu-Sheng Lee "*Distribution Network Reconfiguration for Loss Reduction by Hybrid Differential Evolution*", Electric Power Components and Systems, Vol:33,Issue:12,Pg no:1297-1312, 2005.

[15]. R. Storn and K. V. Price, "*Minimizing the functions of the ICEC'96 contest by differential evolution*," Proc. IEEE on Evolutionary Computation Conf., pp. 842–844, 1996.

[16]. J. P. Chiou and F. S. Wang, "*A hybrid method of differential evolution with application to optimal control problems of a bioprocess system,*" Proc. IEEE on Evolutionary Computation Conf., pp. 627–632, 1998.

[17]. Ji-Pyng Chiou, Chung-Fu Chang, and Ching-Tzong Su.*"Variable Scaling Hybrid Differential Evolution for Solving Network Reconfiguration of Distribution Systems*" IEEE transactions on power systems, vol. 20, no. 2, may 2005.

[18].J. P. Chiou and F. S. Wang, "*Hybrid method of evolutionary algorithms for static and dynamic optimization problems with application to fed-batch fermentation process*," *Comput Chem. Eng.*, vol. 23, pp.1277–1291, 1999.

[19]. T. Back, F. Hoffmeister, and H. P. Schwefel, "*A survey of evolution strategies*," in Proc. Fourth Int. Conf. Genet. Algor., 1991, pp. 2–9.

[20].T. Back and H. P. Schwefel, "*An overviewof evolutionary algorithms for parameter optimization*," *Evol. Comput.*, vol. 1, no. 1, pp. 1–23, 1993.

[21].Martins F. "*Tuning PID controllers using the ITAE criterion*". Int J Eng Educ 2005;21(5):867.

[22].Maiti D, Acharya A, Chakraborty M, Konar A, Janarthanan R. "*Tuning PID and pikdd controllers using the integral time absolute error criterion*". In: 4th International Conference on Information and Automation for Sustainability.ICIAFS 2008; 2008. p. 457–462.

[23].*IEEE standard for interconnecting distributed resources with electric power systems*. IEEE Std 1547-2003.

[24].R. Storn and K. V. Price, "*Minimizing the real function of the ICEC'96contest by differential evolution*," in Proc. IEEE Conf. Evol. Comput.,Nagoya, Japan, 1996, pp. 842–844.